ACS EARTH AND SPACE CHEMISTRY

http://pubs.acs.org/journal/aesccq

Article

Carbon on the Ocean Surface: Temporal and Geographical Investigation

Abigail A. Enders, Scott M. Elliott, and Heather C. Allen*

Cite This: *ACS Earth Space Chem.* 2023, 7, 360−369

Read Online

ACCESS | Metrics & More | Article Recommendations | Supporting Information

ABSTRACT: The sea surface nanolayer (SSnL) is enriched with lipids and proteins; working together, these macromolecules create a unique region between the atmosphere and ocean. Lipids and proteins affect the ocean's surface chemistry, which causes surface tension suppression. Carbon enrichment is ultimately reflected in organic sea spray aerosols and wave damping mechanisms that impact micrometeorology. In the present work, we calculate and examine carbon in the SSnL with a global analysis of carbon that incorporates organic surfactant dynamics. Our carbon estimates are based on chlorophyll distributions deduced from Energy Exascale Earth System Model output data. We assume that chlorophyll can approximate phytoplankton and that phytoplankton are primary contributors to the dissolved organic carbon (DOC) pool. The model calculates the carbon concentration from phytoplankton and zooplankton concentrations, fits a Langmuir isotherm to determine fractional surface coverage, and converts from the fractional coverage to a mass using surface excess to estimate carbon in the SSnL. Organic geochemical diversity of the ocean surface is evidenced by monthly variability and global differences among carbon averages. The model is an estimation of carbon because of the limited data for carbohydrate co-adsorption and molecular behavior of the DOC and particulate organic carbon (POC) pool, but our results can be used as a benchmark throughout future works. Our results reveal large seasonal shifts across the major biomes and among regional interfacial totals. However, the total mass of ~10^{-4} gigatons does not change significantly throughout the year. We propose based on our results that adsorptive equilibria control the organic content of the nanolayer. To the best of our knowledge, these calculations constitute the first example of SSnL organic carbon integrations performed on a planetary scale.

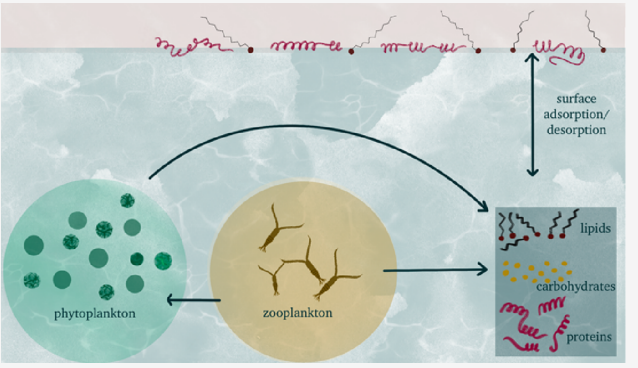

KEYWORDS: *ocean surface chemistry, sea surface nanolayer (SSnL), surfactants, proteins, lipids, global models*

INTRODUCTION

Carbon is the single most essential element for existence of life on Earth.[1] From the polymeric backbone support of diverse biomacromolecules to the varietal self-bonding of which this atom is capable, its impact seems almost infinite.[1−3] This is especially true when considering the effect of increased atmospheric gas concentrations on Earth as a unified ecosystem.[4,5] Since the Industrial Revolution, global usage of fossil fuels has steadily increased.[6,7] A clear display of increased carbon consumption over the last few decades is the stark rise in atmospheric carbon dioxide; CO_2 is the thermochemical fate for all hydrocarbons in the oxidizing atmosphere.[8] Prior to the 1850s, the global concentration of CO_2 was around 280 ppm, but by November of 2020, measurements exceeded 410 ppm.[9] While terrestrial sources of carbon are primarily anthropogenic,[6] the ocean also has a vital role in the carbon cycle through several biogeochemical mechanisms.

Relative to geocycling, emphasis is frequently placed on ocean acidification since the dominant aqueous form of CO_2 is carbonic acid.[10] Yet, the relationship between carbon and Earth's ocean is multi-faceted. Seawater is both a sink and source for carbon because of uptake and return by aquatic organisms extending from mixed layer depths to the sea surface and beyond (Figure 1a,b).[11] The sea surface nanolayer (SSnL) is about 1 nm of thickness (i.e., the thickness of one molecular layer) and is the topmost surface of the sea surface microlayer (SSML, ~1−1000 μm thickness). The SSnL is enriched in organic molecules due to their hydrophobic or hydrophillic properties, and these molecules tend to form in an ordered layer at the ocean surface in a monolayer; the carbon within this monolayer is what we model globally. Since the 1960s, enrichment of organics in the SSML and SSnL has been evidenced by analyses of proteins, lipids, and carbohydrates

Received: August 12, 2022
Revised: December 14, 2022
Accepted: January 4, 2023
Published: January 17, 2023

https://doi.org/10.1021/acsearthspacechem.2c00248
ACS Earth Space Chem. 2023, 7, 360−369

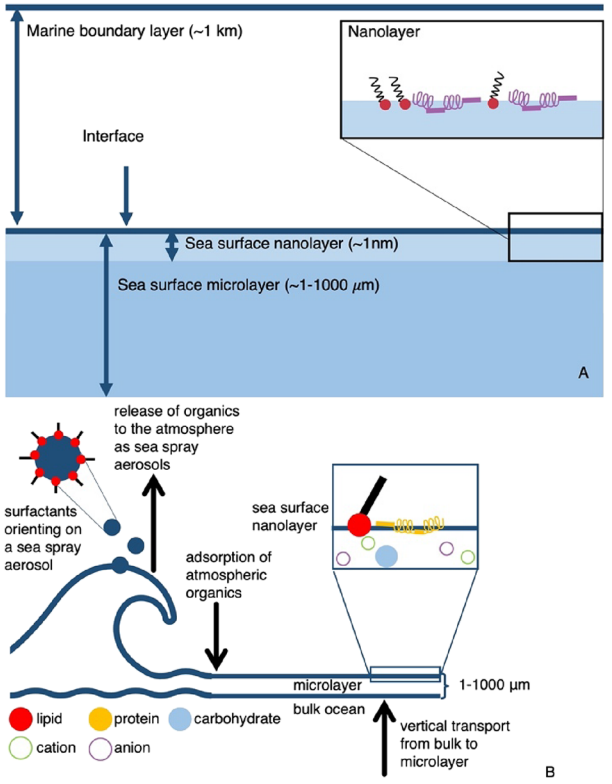

Figure 1. Simplified schematics illustrating (a) relationships between the marine boundary layer (white), sea surface nanolayer (light blue), and sea surface microlayer (dark blue) and (b) highlighting some of the major oceanic processes that occur including vertical transport from the bulk, enrichment of organics at the surface nanolayer, adsorption of atmospheric aerosols and gases, and release of sea spray aerosols from the ocean to the atmosphere.

throughout multiple field studies[12−14] and laboratory experiments.[15−20] However, precise organic composition is difficult to characterize for many reasons, including variable biogeochemistry and transport dynamics within the SSML and SSnL.

Research into the carbon present in the SSML and SSnL is either from field measurements or models that use satellite data or field data to map global estimates.[21−25] We invoke a previously established method of using phytoplankton from chlorophyll satellite data to model carbon.[26] We present a method to calculate net amounts of carbon resident in the SSnL utilizing the Energy Exascale Earth System Model (E3SM) model output; our results are reported as normalized carbon and the well-known global budgeting unit of gigatons. Our effort is equally complicated and enriched by the ocean's inherent biogeographical diversity; details of which are directly reflected in the SSML and SSnL.[27,28] We estimate the overall SSnL mass as a reference through the implementation of previously defined physicochemical properties of the air−sea interface. Specifically, we apply Gibb's equations for surfactant thermodynamics utilizing a modified Langmuir isotherm expression,[29] the concept of an oceanic equation of state,[30] and equilibrium expressions for adsorption and desorption of complex organics at air−liquid interfaces.

Our model parameterization is highly simplified and thus, we acknowledge that the carbon distributions used here are not fully consistent with the reported DOC and POC pools and their surface prevalence. This disconnect is unavoidable. Specifically, there is a knowledge gap in knowing adsorption properties of the total DOC and POC pools because of the inherent dynamic nature of the ocean and the chemical complexity of the pools. For the first modeling attempt in the present work, we assume that the DOC and POC pools retain properties like their initial biomolecular forms in phytoplankton such that a carbon distribution of 60% protein and 20% lipid exists. Our percentages do not explicitly account for the lifetime, decay, or the resultant aged products and the effect that it has on surface activity or enrichment in general. For example, we assume lifetimes of lipids and proteins based on literature values.[31] Depending on the conditions, the decay rate can vary significantly as presented by Duffy and colleagues for proteins[32] and He et al. reported decay rates under hypoxic conditions.[33] There are limitations with that assumption because we know from the literature that lipids, proteins, and carbohydrates are broken down at different rates,[34] and future work will have to refine and improve our model as more data is published. The model we have developed herein requires these fundamental assumptions, as described, to result in a global approximation of SSnL carbon.

Two specific compounds serve as proxies for the protein and lipid adsorptive contributions, bovine serum albumin and stearic acid. We explicitly address the cyclic nature of marine biogeochemical underpinnings; growth, conservation, release, and equilibrium-adsorptive reorganization are simulated for the organic composition of our model nanolayer. Moreover, all quantities are subject to geographic and temporal scaling. Calculated values are compared to total global carbon budgets to provide a perspective on the influence of contributions from biomacromolecules when constrained to the ocean SSnL. Our model values represent an estimation of the global carbon because we only include two molecular classes. To the best of our knowledge, these computations are the first of their kind and they represent a unique portrait of the marine SSnL, the topmost surface layer of the SSML. Overall, we provide insight into the variability of the ocean nanolayer chemistry on a global scale.

METHODS

For our model approximation of carbon in the SSnL, we use an assembly of proteins and lipids, which all enrich this region of the ocean. We identify these components based on the experimental evidence from Cochran et al.,[35] Schiffer et al.,[36] and Pham et al.,[37] among other literature in the field. Specifically, sea spray aerosol formation is dependent on the SSnL and SSML composition, which we are focused on; Cochran and colleagues identify almost 300 surfactants that are best classified as lipids.[35] A work conducted by Schiffer et al. and Pham et al. investigated the biological impact on sea spray aerosols, providing us with a framework to understand how the SSnL is influenced by marine biology.[36,37]

Enrichment of the SSnL occurs, in large part, because of gas and liquid interfacial phenomena; that is, unfavorable interactions between non-polar, carbon-rich organics, and polar water.[29,38] The protein and lipid concentrations are driven by their release from phytoplankton. Here, we use a simplified model system consisting of proteins and lipids as a baseline. From that baseline, we then scale up to a global representation to provide flexible estimates for carbon mass in the SSnL.

Proteins. Proteins are a common exudate or lysate from aquatic species. They are primarily injected into the water

https://doi.org/10.1021/acsearthspacechem.2c00248
ACS Earth Space Chem. 2023, 7, 360−369

Table 1. Summary of Variables Used in Calculation of Total Surface Carbon Mass Including Relevant References for Literature Values

variable	description	value	unit	reference
i	component molecule	1 = protein; 2 = lipid		
C_i	carbon atom concentration of the ith molecule	calculated	μM carbon	
g	zooplanktonic growth rate	1.0	day^{-1}	Sarmiento et al.[56]
C_z	concentration of carbon within zooplankton	calculated	μM carbon	Gibson et al.[48]
C_p	concentration of carbon within plankton	calculated	μM carbon	Gibson et al.[48]
K_{inges}	half saturation of ingestion	7.0	μM carbon	Sarmiento et al.[56]
γ	assimilation efficiency	0.75		Sarmiento et al.[56]
$p_{i,\%}$	percentage of macromolecule within the SSnL	$p_{1,\%} = 60$; $p_{2,\%} = 20$		Elliott et al.[30]
τ_i	lifetime of the molecule	$\tau_1 = 10$; $\tau_2 = 2$	day	Ogunro et al.[31]
$C_{i,ref}$	half saturation carbon atom concentration for the ith molecule	$C_{1,Ref} = 10$; $C_{2,Ref} = 0.5$	μM carbon	Elliott et al.[30]
n_i	effective shape of adsorption isotherm	$n_1 = 0.5$; $n_2 = 1$		Elliott et al.[30]
θ_i	fractional surface coverage for the ith molecule	calculated		
M_{surf}	carbon in the SSnL	calculated	g carbon	
A_{pixel}	surface area of a pixel	$\sim 10^{10}$	m^2	
Γ_i	maximum surface excess of the ith molecule	$\Gamma_1 = 2 \times 10^{-3}$; $\Gamma_2 = 2.5 \times 10^{-3}$	g/m^2	Graham and Phillips[18]

column when organisms are disrupted by grazing or senescing.[16] Graham and Phillips investigated the behavior of three model proteins: β-casein, bovine serum albumin, and lysozyme, with data taken relative to laboratory air−water interfaces.[18] Their results indicate a partly irreversible adsorption of proteins to the air−sea interface but with two-phase equilibration occurring as well and the total resulting in a surface pressure maximum of 20 mN/m and film thicknesses of up to 50−60 Å. Certain processes, such as salting-out, which we expect to occur, can result in greater SSnL coverage and a lowering of measured surface tension (increased surface pressure).[39,40]

Lipids. Lipids, such as fatty acids, phospholipids, and cholesterol, disrupt the surface tension of water through specific amphiphilic enrichment.[29,38] The non-polar tail chains of fatty acids, for example, orient into the air while polar headgroups interact with water itself resulting in a stable monolayer.[41] Headgroups also interact with inorganic cations, further stabilizing the organic films in the SSnL.[42,43] A characteristic monolayer (one molecule thickness) of stearic acid on pure water can reach surface pressures upward of 65−70 mN/m.[44] Organic films tend to stabilize and calm rough seas through their capacity to dampen waves. Wave breakage is a source of bubble bursting and aerosolization of surfactants.

Carbohydrates. Carbohydrates are more soluble and less surface active in aqueous solutions relative to proteins or lipids, but they are still observed in the interfacial region, particularly in the SSML, although it is debated as to its concentration in the SSnL.[15,45,46] Satellite[22] and field[47] studies suggest that carbohydrates are an estimated 20% of the dissolved organic carbon (DOC) in the SSML.[46] By comparison and on an absolute basis, carbohydrate adsorption is weak. Only through processes such as co-adsorption are carbohydrates significantly adsorbed to the SSnL.[45,46] Burrows et al. were able to connect the co-adsorption process through a two-layer Langmuir model for fractional surface coverage that ultimately improves their sea spray model.[20] There are no well-accepted satellite proxy data for the co-adsorption in the presence of mixed monolayers to establish carbohydrate SSnL concentrations; therefore, we must neglect their net contributions. We acknowledge that their presence and geochemical role is non-negligible and should be incorporated in the future after further laboratory experiments on mixed monolayer co-adsorption have been validated. Thus, our estimate is likely limited in establishing total carbon.

Chlorophyll Data and Plankton Concentration. Chlorophyll is monitored at the planetary scale by several satellite instruments (e.g., NASA MODIS) and modeled through E3SM, among others. Model output is compared to chlorophyll satellite data to confirm its accuracy.[48] Monthly averages provide a convenient means to understand geographic and seasonal variability of upper ocean biomass. Phytoplankton are the "primary producers" of the sea, and cell densities are proportional to remotely measured chlorophyll. Specifically, pigments are essential to the photosynthetic process; light-absorbing conjugated bond systems constitute a relatively constant proportion of intracellular compounds. Autotrophs can only live near the ocean surface because of the obligate need for sunlight.[39] Dissolved organic carbon primarily originates from primary production.[22,24,49−51] The literature suggests that using chlorophyll to model carbon and phytoplankton is a viable approach.[22,31,51−55]

Carbon Calculations. All calculations and figures were done using Python scripts. E3SM chlorophyll data were averaged per month for 2005 on a scale of approximately 0.5 by 1° latitude by longitude, respectively.[48] The satellite results are converted from chlorophyll to planktonic carbon concentration (C_p) using the standard ratio of 50:1 (planktonic C to chlorophyll by mass in grams).[52] The ratio is an imperfect representation of all phases of plankton blooms, and we assume carbon averages across a bloom to the defined ratio. Equation 1 accounts for several ocean biogeochemical dynamic processes and ultimately provides a dissolved carbon concentration (C_i) for the ith biomacromolecule. Here, $i = 1$ for protein and $i = 2$ for lipid, but this vector can be expected to lengthen in future studies to account for the diverse chemical pool. The zooplankton maximum growth rate (g) is estimated from literature values,[56] and zooplankton (C_z) values were obtained from E3SM output.[48]

The consumption of phytoplankton due to grazing is limited on a kinetic basis and is accounted for through the relationship $(C_p/(K_{inges} + C_p))$, where K_{inges} is the half saturation constant for ingestion by zooplankton. We adopt rough global average values for key variables (i.e., K_{inges}, τ) established in early ocean models.[56] The local concentration of carbon is further modulated by grazing assimilation efficiency (γ), and steady

https://doi.org/10.1021/acsearthspacechem.2c00248
ACS Earth Space Chem. 2023, 7, 360−369

state is achieved with the mixed layer lifetime (τ) of the ith species. Lastly, we address the fraction or percentage of each molecule (protein and lipid) initially residing in an autotrophic cell. Using literature values, we approximate the carbon associated with proteins and lipids ($p_{i,\%}$) to be 60 and 20% of biomass, respectively.[30] The parameters used are summarized in Table 1.

$$C_i = gC_z\left(\frac{C_p}{K_{inges} + C_p}\right)(1-\gamma)\tau_i p_{i,\%} \quad (1)$$

The conversion from the concentration to SSnL mass requires realistic models of molecular adsorption to the air−water interface. Classic Langmuir isotherms are capable of modeling relevant population competition to zeroth order.[38] Extending beyond the idealization of Langmuir allows us to account for deviations in isothermal surface excess between proteins and lipids, which are attributable to bonding, functionality, and site configuration. We assume that partial coating of the SSnL is limited to one molecular thickness.[29,38,57] Several literature equilibrium constants are adopted in the form of inverse half saturation carbon atom concentrations as a first approximation.[30] The expressions we use are derived from typical laboratory adsorption isotherm behaviors so that the monolayer can be modeled as accurately as possible. An effective fractional surface coverage relevant to the excess is determined via the following relationship:

$$\theta_i = \frac{(1/C_{i,ref})^{n_i} \times (C_i)^{n_i}}{1 + \sum_{i=1}^{2}(1/C_{i,ref})^{n_i} \times (C_i)^{n_i}} \quad (2)$$

Here, $C_{i,ref}$ is the half saturation carbon concentration of the ith biomacromolecule (1 = proteins and 2 = lipids) and noting as stated above that there is no established literature value of $C_{i,eef}$ for carbohydrates. The variable n_i is an adjustable coverage parameter permitting us to set the isotherm shape to typical experimental adsorption curves for each species, and C_i is the calculated bulk seawater carbon concentration of the ith contributor.

The calculations are performed over the entire global ocean, distributed about every one-half degree latitude and one degree longitude. We assume that local marine biogeochemical dynamics are at steady state on this scale because horizontal diffusivities are about 3×10^7 cm^2/s.[58] Results are also grouped by the Longhurst province to summarize SSnL carbon masses regionally.[27] The nanolayer total is determined using a summation over each calculated value (eq 3, see Table 1 for definitions). Our calculations encompass biogeochemical diversity using chlorophyll-a modeling, zooplankton concentrations, and grazing rates of the upper ocean while also presenting integrated amounts in a concise form. The total SSnL mass for each evaluated month is presented in gigatons (Gt) of carbon to provide a convenient reference for comparison to budget figures.

$$\sum_{lat}\sum_{long}\sum_{i} A_{cell}\Gamma_i\theta_i = M_{C,SSnL} \quad (3)$$

Areas are scaled appropriately to the cosine of latitude so that they decrease toward the poles. Based on the model results and excess maxima for surrogate proteins and lipids, we present SSnL carbon estimates. Parameter values inserted into the described equations are presented in Table 1 with relevant references. Maps are normalized to the largest observed value of carbon overall such that the most intense value is calculated as one.

RESULTS AND DISCUSSION

The carbon SSnL mass is estimated to compare to global budget values, with potential to improve the current understanding of how the surface modulates gas transfer, micrometeorology, and global biogeochemistry. Using established relationships between chlorophyll and phytoplanktonic production and consumption, model measurements are converted to dissolved concentrations of carbon for proteins and lipids, the major marine surfactants. Maps of carbon after calculating eq 1 are presented in the SI; these reflect the calculation of C_i for lipids and proteins. Fractional surface coverage is also mapped for each month (SI).

We first compare our calculated concentrations of lipids and proteins (from eq 1) to field measurements of DOC to confirm that our model is representative of physical measurements; these values do not take into account surface adsorption and are not representative of the SSnL.[21] Briefly, we sum over C_i for a given pixel to give us lipid and protein mass and we average over the year to get an estimated carbon concentration. We confirm that our calculated carbon concentrations are close to experimentally determined DOC concentrations, indicating that the model methods are sufficient for global analysis, albeit an underestimate compared to results from Romankevich and Ljutsarev[59] and Rossel and colleagues,[21] as shown in Figure 2.

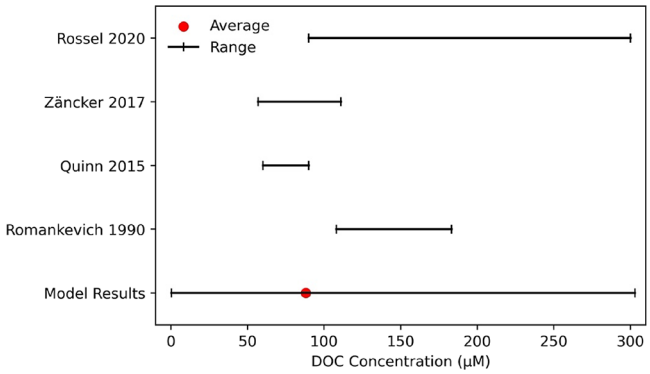

Figure 2. Comparison of four field studies of DOC concentrations[21,59−61] and the range of carbon each month in the region of 0−10 east longitudes and 78−80 north latitudes, which aligns with the regions studied in the Rossel et al. study. The average is calculated for this study over all months for the year of 2005. Ranges are presented for the field study results for more accurate comparison with the model results.

Field measurements of DOC were determined in a multitude of manners throughout the studies that are referenced in Figure 2. Romankevich and Ljutsarev measured DOC off the coast of Peru, in the Bay of Bengal, Philippine Sea, and Weddell Sea (Antarctica) using a four-part system that consisted of oxidation, gas purification, colorimetric titration, and, lastly, a detector.[59] Rossel and colleagues used solid-phase extraction to collect DOC from the Fram Strait over two summers and performed FT-ICR-MS analysis on their extracts.[21] Zäncker and colleagues collected samples off the coast of Peru and used a similar solid-phase extraction procedure as the Rossel study.[61] The results presented in the review by Quinn et al. are a summary of several studies that collected sea water and measured DOC concentrations.[60] The

https://doi.org/10.1021/acsearthspacechem.2c00248
ACS Earth Space Chem. 2023, 7, 360−369

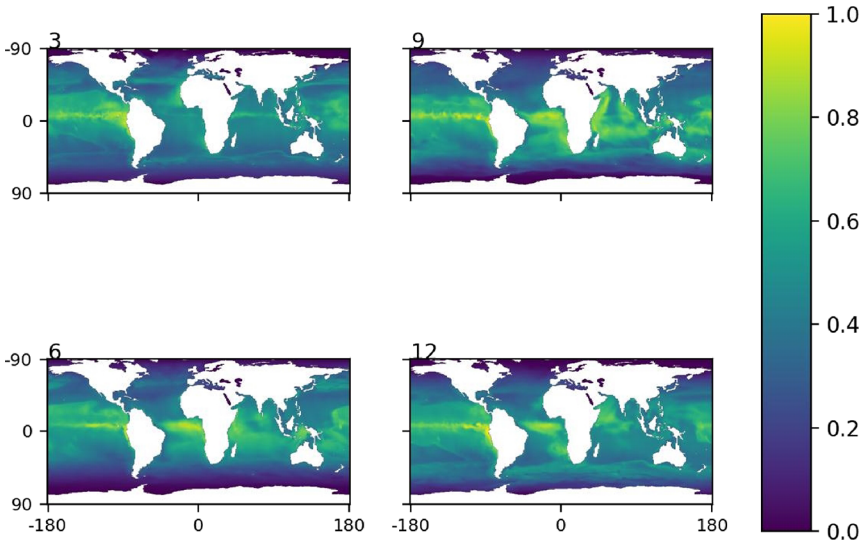

Figure 3. Maps of normalized SSnL carbon for the months of March (3), June (6), September (9), and December (12) from E3SM output for the year 2005 are presented. Normalization is to the greatest observed mass over all months such that 1 is the greatest observed value.

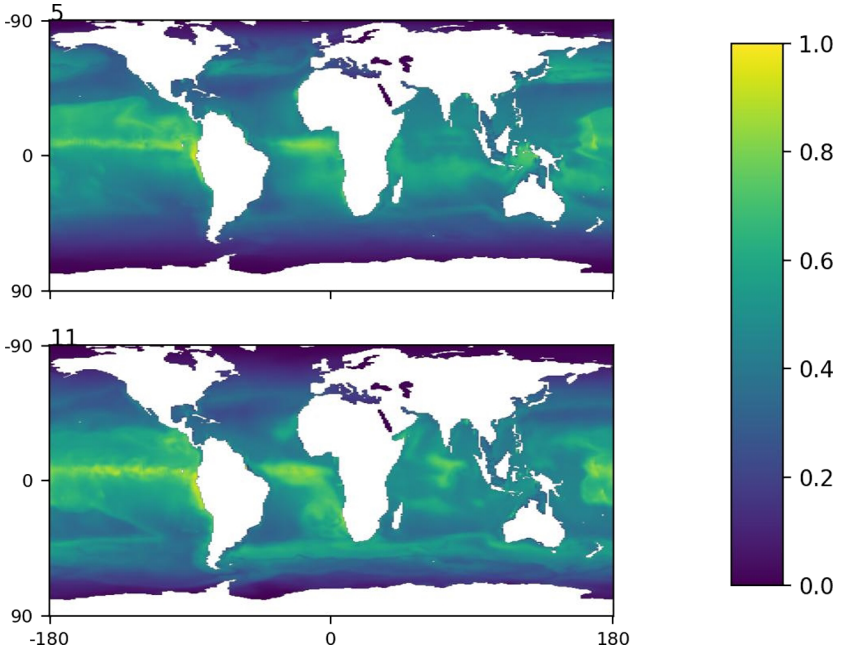

Figure 4. Normalized SSnL carbon for May 2005 (top, "5") and November 2005 (bottom, "11") calculated from E3SM chlorophyll-a and zooplankton output.

presented DOC concentrations from each of these studies is the range such that the lowest reported concentration is the lowest observed value from the study. It would be misleading to present an average as the studies vary geographically and temporally. Our calculated estimate for DOC is reported in the same fashion. The lowest observed value is from winter months (Northern Hemisphere), and high carbon estimates are conversely from summer months, with the average presented as a reference for yearly comparison.

Experimental amounts of DOC are likely divergent from our calculations for two main reasons. Our calculations do not include carbohydrate contributions because of insufficient information about their surface adsorption kinetics, so these calculations have not been included in our model. Second, the dates studied vary. Our model, for example, is for the year 2005. However, the field studies are from a range of years. DOC is dynamic and varies throughout the day, let alone yearly, as observed in the variable standard deviation range from the yearly average. Despite the variations, our calculated value from the modeled carbon is close to field observations of DOC concentrations, which confirms that our approach of using chl-a is viable for modeling applications.

SSnL adsorption is accounted for through experimental isotherm relationships to calculate the fractional carbon coverage. Total carbon mass of the SSnL for a one-month average is determined to be $\sim 10^{-4}$ Gt, indicating simultaneously that there is significant amount of carbon, but that amount is small relative to other contributions in the biogeochemical cycle. For example, most recently in 2020, total CO_2 emissions were estimated at 10.2 Gt carbon and the

https://doi.org/10.1021/acsearthspacechem.2c00248
ACS Earth Space Chem. 2023, 7, 360−369

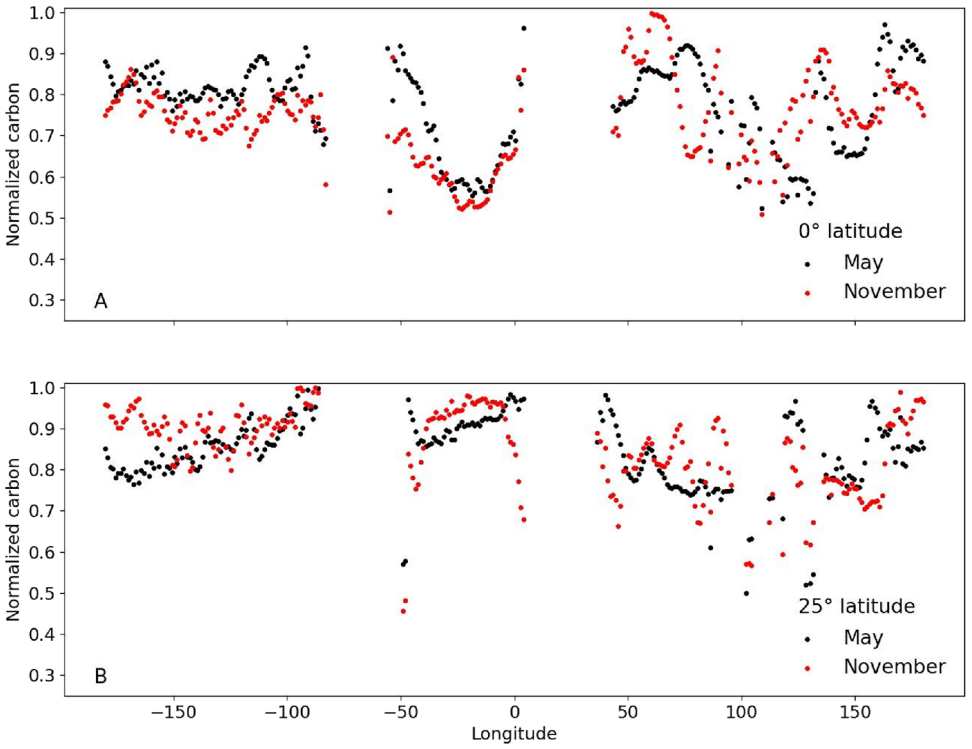

Figure 5. Normalized SSnL carbon across (A) 0° and (B) 25° north latitudes for May and November 2021. Only locations where estimates are greater than zero are included (plots exclude land). Less seasonal variability is observed at the equator in A, and coastal regions in B are well emphasized by the uptick in calculated surface carbon. As we approach land, carbon increases and then decreases in more open ocean regions.

carbon sink into the ocean was about 3 Gt.[7] Carbon in the SSnL is normalized to its greatest single pixel value; $\sim 10^7$ g carbon is represented by a value of 1 and bright yellow regions on maps. Results for all months are mapped to emphasize the variability throughout the calendar year (SI).

We observe the seasonal variability more closely in the months of change (Figure 3). Maps for March, June, September, and December emphasize the hemisphere separation and seasonality. In June and September, southern oceans are significantly darker blue/purple, which is indicative of less carbon in the southern hemisphere winter and spring. The equator is defined by consistently high values of carbon, but seasonal variations are still observed, most notably between March and December. May and November 2005 monthly averages provide Northern Hemisphere mid-spring and mid-fall references, with 6 months of separation (Figure 4).

Our results indicate that coastlines support higher carbon biomass, which is supported by literature observations reported for field studies.[28] For example, the yellow-green coloring offshore Chile is consistent with well-known eastern basin upwelling and associated biological activity. Similarly, regions of remote open ocean exhibit significantly lower masses in their respective fall seasons, and this can be seen most notably by contrasting May and November shifting central minimum of the South Pacific and North Pacific Gyres. Even equatorial variability and continuity are of significance (Figure 5a). The equator has a more constant yearly temperature and increased upwelling of nutrients through ocean circulation, which creates ideal conditions for marine biota to thrive and ultimately produce more carbon (bright yellow on maps).

Figure 5a,b emphasizes longitudinal variability and a degree of similarity between the two central sample months. Normalized carbon for spring and fall is overlaid for latitudes of 0 and 25°. Regional overlap of red and black is an indication that SSnL carbon remains consistent over time. Figure 5a highlights the detailed seasonal variability we observe along the equator. Carbon mass is lower in May when viewed along this longitudinal axis. Greater November SSnL carbon is explained by the behavior of global trade winds.

As the adjoining hemispheres move in and out of summer/winter, the carbon mass rises and falls by 5% or more (Figure 5). As summer ends in the two hemispheres, low-latitude aquatic productivity increases since there is more upward-mixing, resulting in injection of nutrient materials. This ultimately contributes to a relatively concentrated SSnL. In the mid-range Northern Hemisphere (above 40° latitude), carbon decreases from May to November and this effect is driven by the standard productivity decreases; seasonal algal blooms do not persist into late fall. This is supported by the higher masses around −40° (southern hemisphere) in November relative to May.

At 25° north latitude, Figure 5b, we observe greater carbon mass in northern hemispheric spring across most longitudes. November displays lower or unchanged surface carbon between the two sample months. There are few longitudes where northern November outpaces May at this selected mid-latitude, mostly occurring in coastal areas. Our observations confirm regular oceanographic seasonal variations known to modulate the contemporary distribution of primary productivity. For example, as the Northern Hemisphere approaches summer, a strong upwelling of nutrients becomes stabilized in the mixed layer. Combined with seasonally increased temperature and daylight hours, this change gives rise to plankton blooms and the ecosystem is subsequently enriched with carbon.

https://doi.org/10.1021/acsearthspacechem.2c00248
ACS Earth Space Chem. 2023, 7, 360−369

Calculated masses were evaluated over the named ecological regions defined by Longhurst in order to evaluate biome diversity because the sum total global SSnL carbon does not vary seasonally (Figure 6).[27] Regional mass totals summarize

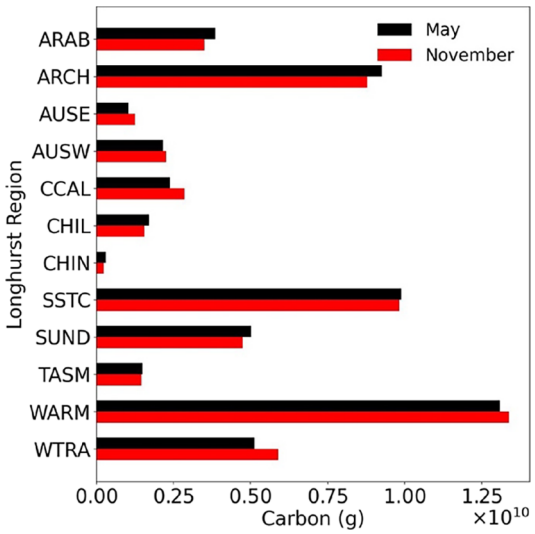

Figure 6. Subset of Longhurst regions with SSnL carbon mass (g) between May and November 2021. Regions are ordered alphabetically by their four-letter standard codes. All values are presented in the SI, and a subset is discussed in the text to underscore key observations. Province acronyms are defined as follows: Northwest Arabian Sea Upwelling (ARAB), Archipelagic Deep Basins (ARCH), East Australian Coastal (AUSE), Western Australian and Indonesian Coast (AUSW), California Current (CCAL), Chile Current Coastal (CHIL), China Sea Coastal (CHIN), South Subtropical Convergence (SSTC), Sunda-Arafura Shelves (SUND), Tasman Sea (TASM), Western Pacific Warm Pool (WARM), and Western Tropical Atlantic (WTRA).

month to month variability. Observed carbon decreased in the Northwest Arabian Sea upwelling province (ARAB) from May to November. We also noted a decrease in Western Tropical Atlantic (WTRA) between the selected months. The South Pacific Subtropical Gyre (SPSG) is a relatively biologically quiescent region, but it is vast, so effects are amplified (SI). By contrast, the California current (CCAL) is narrow and restricted but it is subject to coastal nutrient upwelling.

Total SSnL carbon mass was determined by summing over all pixels of non-zero chlorophyll measurements. In both months, the calculated value was $\sim 10^{-4}$ Gt. Monthly variability is minimal when we integrate across the entire globe since the hemispheres offset one another. We observe only a 4% difference. Therefore, the biogeochemically driven variability evidenced by Figures 3−6 is seasonally symmetrical. Ultimately, we attribute consistent carbon concentrations to adsorption equilibria exerting primary control over the ratio of bulk concentration to SSnL carbon.

Due to local seasonal variability shifting globally, the change in individual biomes does not have a strong impact on the global values. Seasonality reflects the geographic scope of mixed layer productivity. The SSnL and SSML reservoirs must possess an ecological geography of their own consistent with several recent regional analyses.[28,30] The results assist in understanding the geocycling of surface pressure (reduced interfacial tension), which likely affects micrometeorological phenomena. From these results, we assert that global fluid dynamic parameters, such as the drag coefficient, are likely highly variable because there is significant carbon at the SSnL.

These carbon enrichments are important to consider alongside other reservoirs within the Earth system due to aerosol composition and boundary layer turbulence through interfacial roughness.[22,24] If the contributions from the SSnL are omitted in determining environmental pathways of carbon, then a planetary self-regulatory mechanism is neglected. We assert that molecules in the SSnL may have critical links between carbon, micrometeorology, biogeochemistry, and climate.

CONCLUSIONS

The role of a carbon-rich region dividing the ocean and atmosphere remained vague in global studies recently despite the tendency of carbon-rich molecules to organize at the SSnL. The ocean surface has unique carbon sequestration capability; therefore, we examined distributions and variability for the regional to global masses involved. Chlorophyll and zooplankton data from E3SM were used to calculate an integrated SSnL carbon mass for proxy compounds selected from among natural proteins and lipids. The computations were controlled by parameterizations for phytoplanktonic (primary) and zooplanktonic (secondary) production. We determined that SSnL carbon varies both temporally and geographically; however, the monthly total remains consistent at approximately 10^{-4} Gt. Emphasis is placed here upon temporal and geographical fluctuations, which are estimated from remotely sensed observations.

The small value we calculate is indicative of a large relative global geocycling impact. The molecular reservoir of the SSnL functions as a direct physical barrier and physicochemical moderator between the ocean and the atmosphere.[16,62−64] For example, the roughness-driven drag coefficient is likely affected by surface pressure since friction elements are reduced in the presence of amphiphilic species. Winds passing over the ocean "grip" the surface less effectively when the chemical complexity is enriched.[65] The local variability of the SSnL thus results in a wide array of effects on global micrometeorology. The SSnL carbon mass is many orders of magnitude less than present day global anthropogenic CO_2 emissions (about 10 Gt).[7] Yet, the thin organic nanolayer[11] appears to control the transfer of organics from the ocean to the atmosphere through aerosols. In aerosols, the organic molecules may act as ice nucleators or cloud condensation nuclei and will become acidified.[66]

Overall, we conclude that impacts of the carbon-enriched SSnL should be more thoroughly investigated. The model presented herein relies heavily on simple assumptions regarding the molecular structure of typical surfactants, chlorophyll-a, and the food web concentrations. We know that the non-equilibrium of the ocean departs from our assumptions. A more complete understanding of organic chemistry focused at the SSnL requires that future iterations address, for example, the variability of phytoplankton taxonomy throughout upper layers, along with detailed species-by-species composition and molecular aging. This would provide greater detail as to how well chlorophyll-a performs as a proxy for biological activity in the model and account for the physical and chemical changes that may be relevant during ecological succession. The model can be expanded upon to develop a model capable of surface tension reduction estimates, which would further advance our understanding of ocean surface chemistry and its effects. The

https://doi.org/10.1021/acsearthspacechem.2c00248
ACS Earth Space Chem. 2023, 7, 360−369

interaction of dissolved and adsorbed carbon through planetary scale surface chemistry is of direct relevance to many aspects of evolving contemporary climate, and we are hopeful that this initial examination of mass variation will provide a starting point.

■ ASSOCIATED CONTENT

Supporting Information

The Supporting Information is available free of charge at https://pubs.acs.org/doi/10.1021/acsearthspacechem.2c00248.

Lipid concentration maps, protein concentration maps, fractional surface coverage maps, carbon SSnL maps (non-normalized), Longhurst region carbon results, and normalized SSnL carbon maps for all months (2005) (PDF)

■ AUTHOR INFORMATION

Corresponding Author

Heather C. Allen − *Department of Chemistry and Biochemistry, The Ohio State University, Columbus, Ohio 43210, United States;* orcid.org/0000-0003-3120-6784; Email: allen@chemistry.ohio-state.edu

Authors

Abigail A. Enders − *Department of Chemistry and Biochemistry, The Ohio State University, Columbus, Ohio 43210, United States*

Scott M. Elliott − *Computational Physics and Methods (CCS-2), Los Alamos National Laboratory, Los Alamos, New Mexico 87545, United States*

Complete contact information is available at: https://pubs.acs.org/10.1021/acsearthspacechem.2c00248

Notes

The authors declare no competing financial interest.

■ ACKNOWLEDGMENTS

A.A.E and S.M.E. acknowledge funding support from the Regional and Global Model Analysis (RGMA) component of the Earth and Environmental System Modeling (EESM) program, within the U.S. Department of Energy's Office of Science. It is a direct contribution to the HiLAT-RASM project. A.A.E. and H.C.A. also acknowledge funding from the National Science Foundation through the Center for Aerosol Impacts on Chemistry of the Environment (CAICE) under grant no. CHE-180197.

■ REFERENCES

(1) Carey, F. A.; Giuliano, R. M. *Organic Chemistry*; 10th ed.; McGraw-Hill Education, 2016.

(2) Carey, F. A.; Sundberg, R. J. *Advanced Organic Chemistry Part A: Structure and Mechanisms*; 5th ed.; Springer US, 2007.

(3) Wade, L.; Simek, J. *Organic Chemistry*; 9th ed.; Pearson, 2016.

(4) NOAA *What is the carbon cycle?* https://oceanservice.noaa.gov/facts/carbon-cycle.html (accessed 2021-12-15).

(5) Taub, D. R. Effects of Rising Atmospheric Concentrations of Carbon Dioxide on Plants. *Nat. Educ. Knowl.* **2010**, *3*, 21.

(6) EPA *Global greenhouse gas emmisions data*; https://www.epa.gov/ghgemissions/global-greenhouse-gas-emissions-data (accessed 2021-12-15).

(7) Friedlingstein, P.; O'Sullivan, M.; Jones, M. W.; Andrew, R. M.; Hauck, J.; Olsen, A.; Peters, G. P.; Peters, W.; Pongratz, J.; Sitch, S.; Le Quéré, C.; Canadell, J. G.; Ciais, P.; Jackson, R. B.; Alin, S.; Aragão, L. E. O. C.; Arneth, A.; Arora, V.; Bates, N. R.; Becker, M.; Benoit-Cattin, A.; Bittig, H. C.; Bopp, L.; Bultan, S.; Chandra, N.; Chevallier, F.; Chini, L. P.; Evans, W.; Florentie, L.; Forster, P. M.; Gasser, T.; Gehlen, M.; Gilfillan, D.; Gkritzalis, T.; Gregor, L.; Gruber, N.; Harris, I.; Hartung, K.; Haverd, V.; Houghton, R. A.; Ilyina, T.; Jain, A. K.; Joetzjer, E.; Kadono, K.; Kato, E.; Kitidis, V.; Korsbakken, J. I.; Landschützer, P.; Lefèvre, N.; Lenton, A.; Lienert, S.; Liu, Z.; Lombardozzi, D.; Marland, G.; Metzl, N.; Munro, D. R.; Nabel, J. E. M. S.; Nakaoka, S.-I.; Niwa, Y.; O'Brien, K.; Ono, T.; Palmer, P. I.; Pierrot, D.; Poulter, B.; Resplandy, L.; Robertson, E.; Rödenbeck, C.; Schwinger, J.; Séférian, R.; Skjelvan, I.; Smith, A. J. P.; Sutton, A. J.; Tanhua, T.; Tans, P. P.; Tian, H.; Tilbrook, B.; Van Der Werf, G.; Vuichard, N.; Walker, A. P.; Wanninkhof, R.; Watson, A. J.; Willis, D.; Wiltshire, A. J.; Yuan, W.; Yue, X.; Zaehle, S. Global Carbon Budget 2020. *Earth Syst. Sci. Data* **2020**, *12*, 3269−3340.

(8) Ritchie, G. *Atmospheric Chemistry*; 1st ed.; WSPC: Europe, 2017.

(9) NOAA *Carbon cycle greenhouse gases*; https://gml.noaa.gov/ccgg/index.html (accessed 2020-12-15).

(10) Jiang, L. Q.; Carter, B. R.; Feely, R. A.; Lauvset, S. K.; Olsen, A. Surface Ocean PH and Buffer Capacity: Past Present and Future. *Sci. Rep.* **2019**, *9*, 1−11.

(11) Engel, A.; Bange, H. W.; Cunliffe, M.; Burrows, S. M.; Friedrichs, G.; Galgani, L.; Herrmann, H.; Hertkorn, N.; Johnson, M.; Liss, P. S.; Quinn, P. K.; Schartau, M.; Soloviev, A.; Stolle, C.; Upstill-Goddard, R. C.; van Pinxteren, M.; Zäncker, B. The Ocean's Vital Skin: Toward an Integrated Understanding of the Sea Surface Microlayer. *Front. Mar. Sci.* **2017**, *4*, 165.

(12) Jarvis, N. L.; Garrett, W. D.; Scheiman, M. A.; Timmons, C. O. Surface Chemical Characterization of Surface-Active Material in Seawater. *Limnol. Oceanogr.* **1967**, *12*, 88−96.

(13) Garrett, W. D. The Organic Chemical Composition of the Ocean Surface. *Deep-Sea Res. Oceanogr. Abstr.* **1967**, *14*, 221.

(14) Barger, W. R.; Garrett, W. D.; Mollo-Christensen, E. L.; Ruggles, K. W. Effects of an Artificial Sea Slick upon the Atmosphere and the Ocean. *J. Appl. Meteorol.* **1970**, *9*, 396−400.

(15) Cochran, R. E.; Jayarathne, T.; Stone, E. A.; Grassian, V. H. Selectivity Across the Interface: A Test of Surface Activity in the Composition of Organic-Enriched Aerosols from Bubble Bursting. *J. Phys. Chem. Lett.* **2016**, *7*, 1692−1696.

(16) Rogers, M. M.; Neal, J. F.; Saha, A.; Algarni, A. S.; Hill, T. C. J.; Allen, H. C. The Ocean's Elevator: Evolution of the Air−Seawater Interface during a Small-Scale Algal Bloom. *ACS Earth Space Chem.* **2020**, *4*, 2347−2357.

(17) Garrett, W. D. Stabilization of Air Bubbles at the Air-Sea Interface by Surface-Active Material. *Deep-Sea Res. Oceanogr. Abstr.* **1967**, *14*, 661−672.

(18) Graham, D. E.; Phillips, M. C. Proteins at Liquid Interfaces. II. Adsorption Isotherms. *J. Colloid Interface Sci.* **1979**, *70*, 415−426.

(19) Neuman, R. D. Stearic Acid and Calcium Stearate Monolayer Collapse. *J. Colloid Interface Sci.* **1976**, *56*, 505−510.

(20) Burrows, S. M.; Ogunro, O.; Frossard, A. A.; Russell, L. M.; Rasch, P. J.; Elliott, S. M. A Physically Based Framework for Modeling the Organic Fractionation of Sea Spray Aerosol from Bubble Film Langmuir Equilibria. *Atmos. Chem. Phys.* **2014**, *14*, 13601−13629.

(21) Rossel, P. E.; Bienhold, C.; Hehemann, L.; Dittmar, T.; Boetius, A. Molecular Composition of Dissolved Organic Matter in Sediment Porewater of the Arctic Deep-Sea Observatory HAUSGARTEN (Fram Strait). *Front. Mar. Sci.* **2020**, *7*, 428.

(22) Roy, S. Distributions of Phytoplankton Carbohydrate, Protein and Lipid in the World Oceans from Satellite Ocean Colour. *ISME J.* **2018**, *12*, 1457−1472.

(23) Arenz, R. F., Jr.; Lewis, W. M., Jr.; Saunders, J. F., III Determination of Chlorophyll and Dissolved Organic Carbon from Reflectance Data for Colorado Reservoirs. *Int. J. Remote Sens.* **1996**, *17*, 1547−1565.

(24) Myklestad, S. M. Dissolved Organic Carbon from Phytoplankton. In *Marine Chemistry*; Wangersky, P. J., Ed.; Springer Berlin

Heidelberg: Berlin, Heidelberg, 2000; pp. 111−148. doi: DOI: 10.1007/10683826_5.
(25) Carlson, D. J. Dissolved Organic Materials in Surface Microlayers: Temporal and Spatial Variability and Relation to Sea State. *Limnol. Oceanogr.* **1983**, *28*, 415−431.
(26) Kasprzak, P.; Padisák, J.; Koschel, R.; Krienitz, L.; Gervais, F. Chlorophyll a Concentration across a Trophic Gradient of Lakes: An Estimator of Phytoplankton Biomass? *Limnologica* **2008**, *38*, 327−338.
(27) Longhurst, A. *Ecological Geography of the Sea*; 2nd ed.; Academic Press, 2006.
(28) Elliott, S.; Burrows, S.; Cameron-Smith, P.; Hoffman, F.; Hunke, E.; Jeffery, N.; Liu, Y.; Maltrud, M.; Menzo, Z.; Ogunro, O.; Van Roekel, L.; Wang, S.; Brunke, M.; Jin, M.; Letscher, R.; Meskhidze, N.; Russell, L.; Simpson, I.; Stokes, D.; Wingenter, O. Does Marine Surface Tension Have Global Biogeography? Addition for the OCEANFILMS Package. *Atmosphere* **2018**, *9*, 216.
(29) Gaines, G. L., Jr. The Thermodynamic Equation of State for Insoluble Monolayers I. Uncharged Films. *J. Chem. Phys.* **1978**, *69*, 924−930.
(30) Elliott, S.; Menzo, Z.; Jayasinghe, A.; Allen, H. C.; Ogunro, O.; Gibson, G.; Hoffman, F.; Wingenter, O. Biogeochemical Equation of State for the Sea-Air Interface. *Atmosphere* **2019**, *10*, 230.
(31) Ogunro, O. O.; Burrows, S. M.; Elliott, S.; Frossard, A. A.; Hoffman, F.; Letscher, R. T.; Moore, J. K.; Russell, L. M.; Wang, S.; Wingenter, O. W. Global Distribution and Surface Activity of Macromolecules in Offline Simulations of Marine Organic Chemistry. *Biogeochemistry* **2015**, *126*, 25−56.
(32) Duffy, M. E.; Adams, C. M.; Homolka, K. K.; Neibauer, J. A.; Mayer, L. M.; Keil, R. G. Degradation of Diatom Protein in Seawater: A Peptide-Level View. *Front. Mar. Sci.* **2022**, *8*, No. 757245.
(33) He, Y.; Sun, C.; Li, W.; Yang, G.-P.; Ding, H. Degradation of Lipids in Seasonal Hypoxic Seawater under Different Oxygen Saturation. *J. Oceanol. Limnol.* **2018**, *36*, 1570−1585.
(34) Benner, R.; Amon, R. M. W. The Size-Reactivity Continuum of Major Bioelements in the Ocean. *Annu. Rev. Mar. Sci.* **2015**, *7*, 185−205.
(35) Cochran, R. E.; Laskina, O.; Jayarathne, T.; Laskin, A.; Laskin, J.; Lin, P.; Sultana, C.; Lee, C.; Moore, K. A.; Cappa, C. D.; Bertram, T. H.; Prather, K. A.; Grassian, V. H.; Stone, E. A. Analysis of Organic Anionic Surfactants in Fine and Coarse Fractions of Freshly Emitted Sea Spray Aerosol. *Environ. Sci. Technol.* **2016**, *50*, 2477−2486.
(36) Schiffer, J. M.; Mael, L. E.; Prather, K. A.; Amaro, R. E.; Grassian, V. H. Sea Spray Aerosol: Where Marine Biology Meets Atmospheric Chemistry. *ACS Cent. Sci.* **2018**, *4*, 1617−1623.
(37) Pham, D. Q.; O'Brien, R.; Fraund, M.; Bonanno, D.; Laskina, O.; Beall, C.; Moore, K. A.; Forestieri, S.; Wang, X.; Lee, C.; Sultana, C.; Grassian, V.; Cappa, C. D.; Prather, K. A.; Moffet, R. C. Biological Impacts on Carbon Speciation and Morphology of Sea Spray Aerosol. *ACS Earth Space Chem.* **2017**, *1*, 551−561.
(38) Davies, J. T.; Rideal, E. K. *Interfacial Phenomena*; 2nd ed.; Academic Press, 1961.
(39) Li, Y.; Shrestha, M.; Luo, M.; Sit, I.; Song, M.; Grassian, V. H.; Xiong, W. Salting up of Proteins at the Air/Water Interface. *Langmuir* **2019**, *35*, 13815−13820.
(40) Duong-Ly, K. C.; Gabelli, S. B. *Salting out of Proteins Using Ammonium Sulfate Precipitation*; 1st ed.; Elsevier Inc.: 2014; Vol. *541*, DOI: 10.1016/B978-0-12-420119-4.00007-0.
(41) Sears, D. F.; Schulman, J. H. Influence of Water Structures on the Surface Pressure, Surface Potential, and Area of Soap Monolayers of Lithium, Sodium, Potassium, and Calcium. *J. Phys. Chem.* **1964**, *68*, 3529−3534.
(42) Zhang, T.; Brantley, S. L.; Verreault, D.; Dhankani, R.; Corcelli, S. A.; Allen, H. C. Effect of PH and Salt on Surface PK a of Phosphatidic Acid Monolayers. *Langmuir* **2018**, *34*, 530−539.
(43) Adams, E. M.; Casper, C. B.; Allen, H. C. Effect of Cation Enrichment on Dipalmitoylphosphatidylcholine (DPPC) Monolayers at the Air-Water Interface. *J. Colloid Interface Sci.* **2016**, *478*, 353−364.
(44) Carter-Fenk, K. A.; Allen, H. C. Collapse Mechanisms of Nascent and Aged Sea Spray Aerosol Proxy Films. *Atmosphere* **2018**, *9*, 503.
(45) Vazquez de Vasquez, M. G.; Rogers, M. M.; Carter-Fenk, K. A.; Allen, H. C. Discerning Poly- and Monosaccharide Enrichment Mechanisms: Alginate and Glucuronate Adsorption to a Stearic Acid Sea Surface Microlayer. *ACS Earth Space Chem.* **2022**, *6*, 1581.
(46) Carter-Fenk, K. A.; Dommer, A. C.; Fiamingo, M. E.; Kim, J.; Amaro, R. E.; Allen, H. C. Calcium Bridging Drives Polysaccharide Co-Adsorption to a Proxy Sea Surface Microlayer. *Phys. Chem. Chem. Phys.* **2021**, *23*, 16401−16416.
(47) Pakulski, J. D.; Benner, R. Abundance and Distribution of Carbohydrates in the Ocean. *Limnol. Oceanogr.* **1994**, *39*, 930−940.
(48) Gibson, G.; Weijer, W.; Jeffery, N.; Wang, S. Relative Impact of Sea Ice and Temperature Changes on Arctic Marine Production. *J. Geophys. Res.: Biogeosci.* **2020**, *125*, No. e2019JG005343.
(49) Biddanda, B.; Benner, R. Carbon, Nitrogen, and Carbohydrate Fluxes during the Production of Particulate and Dissolved Organic Matter by Marine Phytoplankton. *Limnol. Oceanogr.* **1997**, *42*, 506−518.
(50) Kinsey, J. D.; Corradino, G.; Ziervogel, K.; Schnetzer, A.; Osburn, C. L. Formation of Chromophoric Dissolved Organic Matter by Bacterial Degradation of Phytoplankton-Derived Aggregates. *Front. Mar. Sci.* **2018**, *4*, 430.
(51) Legendre, L.; Michaud, J. Chlorophyll a to Estimate the Particulate Organic Carbon Available as Food to Large Zooplankton in the Euphotic Zone of Oceans. *J. Plankton Res.* **1999**, *21*, 2067−2083.
(52) Fasham, M. J. R.; Sarmiento, J. L.; Slater, R. D.; Ducklow, H. W.; Williams, R. Ecosystem Behavior at Bermuda Station "s" and Ocean Weather Station "India:" A General Circulation Model and Observational Analysis. *Global Biogeochem. Cycles* **1993**, *7*, 379−415.
(53) Manning, N. F.; Wang, Y. C.; Long, C. M.; Bertani, I.; Sayers, M. J.; Bosse, K. R.; Shuchman, R. A.; Scavia, D. Extending the Forecast Model: Predicting Western Lake Erie Harmful Algal Blooms at Multiple Spatial Scales. *J. Great Lakes Res.* **2019**, *45*, 587−595.
(54) Engel, A.; Sperling, M.; Sun, C.; Grosse, J.; Friedrichs, G. Organic Matter in the Surface Microlayer: Insights from a Wind Wave Channel Experiment. *Front. Mar. Sci.* **2018**, *5*, 182.
(55) Wakeham, S. G.; Lee, C.; Hedges, J. I.; Hernes, P. J.; Peterson, M. J. Molecular Indicators of Diagenetic Status in Marine Organic Matter. *Geochim. Cosmochim. Acta* **1997**, *61*, 5363−5369.
(56) Sarmiento, J. L.; Slater, R. D.; Fasham, M. J. R.; Ducklow, H. W.; Toggweiler, J. R.; Evans, G. T. A Seasonal Three-Dimensional Ecosystem Model of Nitrogen Cycling in the North Atlantic Euphotic Zone. *Global Biogeochem. Cycles* **1993**, *7*, 417−450.
(57) Rideal, E. K. *An Introduction to Surface Chemistry*; First; Cambridge University Press, 1926.
(58) Matsuzaki, Y.; Fujita, I. In Situ Estimates of Horizontal Turbulent Diffusivity at the Sea Surface for Oil Transport Simulation. *Mar. Pollut. Bull.* **2017**, *117*, 34−40.
(59) Romankevich, E. A.; Ljutsarev, S. V. Dissolved Organic Carbon in the Ocean. *Mar. Chem.* **1990**, *30*, 161−178.
(60) Quinn, P. K.; Collins, D. B.; Grassian, V. H.; Prather, K. A.; Bates, T. S. Chemistry and Related Properties of Freshly Emitted Sea Spray Aerosol. *Chem. Rev.* **2015**, *115*, 4383−4399.
(61) Zäncker, B.; Bracher, A.; Röttgers, R.; Engel, A. Variations of the Organic Matter Composition in the Sea Surface Microlayer: A Comparison between Open Ocean, Coastal, and Upwelling Sites Off the Peruvian Coast. *Front. Microbiol.* **2017**, *8*, 2369.
(62) Cunliffe, M.; Engel, A.; Frka, S.; Gašparović, B.; Guitart, C.; Murrell, J. C.; Salter, M.; Stolle, C.; Upstill-Goddard, R.; Wurl, O. Sea Surface Microlayers: A Unified Physicochemical and Biological Perspective of the Air−Ocean Interface. *Prog. Oceanogr.* **2013**, *109*, 104−116.
(63) Wilson, T. W.; Ladino, L. A.; Alpert, P. A.; Breckels, M. N.; Brooks, I. M.; Browse, J.; Burrows, S. M.; Carslaw, K. S.; Huffman, J. A.; Judd, C.; Kilthau, W. P.; Mason, R. H.; McFiggans, G.; Miller, L. A.; Nájera, J. J.; Polishchuk, E.; Rae, S.; Schiller, C. L.; Si, M.;

Temprado, J. V.; Whale, T. F.; Wong, J. P. S.; Wurl, O.; Yakobi-Hancock, J. D.; Abbatt, J. P. D.; Aller, J. Y.; Bertram, A. K.; Knopf, D. A.; Murray, B. J. A Marine Biogenic Source of Atmospheric Ice-Nucleating Particles. *Nature* **2015**, *525*, 234−238.
(64) Cochran, R. E.; Laskina, O.; Trueblood, J. V.; Estillore, A. D.; Morris, H. S.; Jayarathne, T.; Sultana, C. M.; Lee, C.; Lin, P.; Laskin, J.; Laskin, A.; Dowling, J. A.; Qin, Z.; Cappa, C. D.; Bertram, T. H.; Tivanski, A. V.; Stone, E. A.; Prather, K. A.; Grassian, V. H. Molecular Diversity of Sea Spray Aerosol Particles: Impact of Ocean Biology on Particle Composition and Hygroscopicity. *Chem* **2017**, *2*, 655−667.
(65) Peixoto, J.; Oort, A. *Physics of Climate*; 1st ed.; Springer US.
(66) *Acidity across the interface from the ocean surface to sea spray aerosol*; PNAS. DOI: 10.1073/pnas.2018397118 (accessed 2022-07-28).

https://doi.org/10.1021/acsearthspacechem.2c00248
ACS Earth Space Chem. 2023, 7, 360−369